Acta Crystallographica Section A
**Foundations of Crystallography**
ISSN 0108-7673

Received 7 June 2000
Accepted 20 July 2000



# The crystallite size–disorder relationship based on the spiral paracrystal

**J. L. Eads and R. P. Millane***

Whistler Center for Carbohydrate Research, and Computational Science and Engineering Program, Purdue University, West Lafayette, IN 47907-1160, USA. Correspondence e-mail: rmillane@purdue.edu

A simple physical model of the relationship between crystallite size and disorder for paracrystalline materials is presented, based on the spiral paracrystal and distortion of the lattice cells. Simulations show that the model leads to relationships similar to the $\alpha^*$ rule. Average crystallite sizes predicted by the model are in agreement with experimental data and also allow crystallite-size distributions to be proposed. The model provides a more satisfactory and complete explanation of this relationship than do current descriptions.

## 1. Introduction

Disordered crystalline materials are ubiquitous in nature and technology, and X-ray diffraction is an important means of analyzing such materials (Welberry, 1985; Stroud & Millane, 1995). Performing such an analysis requires both a statistical model of the disordered system and a method for calculating diffraction patterns based on the model. Models of crystalline disorder are therefore useful in both the description of such materials and analysis of their diffraction data. X-ray diffraction analysis shows that the average size of the crystalline domains of materials incorporating cumulative, or paracrystalline, disorder is inversely related to the degree of disorder in the specimen (this relationship is sometimes called the '$\alpha^*$ rule') (Hosemann & Hindeleh, 1995). We examine here this relationship in terms of a model based on the spiral paracrystal.

Disordered crystalline systems can be conveniently described in terms of *lattice disorder* and *substitution disorder*. Substitution disorder consists of variations in the units (different atoms or molecules, or different orientations of the same molecule) located at each site of the crystal lattice. Lattice disorder consists of variations in the positions of the lattice sites away from those of an ordered periodic lattice. Obviously, substitution disorder usually induces some degree of lattice disorder. We restrict ourselves here to lattice disorder (without considering the underlying basis for the disorder). The simplest model of lattice disorder involves independent distortions of the lattice sites away from those of a regular periodic lattice. This is referred to as thermal disorder, disorder of the *first kind* (Hosemann & Bagchi, 1962) or uncorrelated disorder (Stroud & Millane, 1996), and, although it is useful in many situations (Millane & Stroud, 1991; Stroud & Millane, 1995), it does not incorporate the dependence between distortions at neighboring lattice sites (*i.e. correlated* disorder) that are often characteristic, at least to some degree, of close-packed systems. Correlated disorder can be detected and characterized experimentally since it results in X-ray diffraction patterns whose peaks broaden with increasing scattering angle, whereas for uncorrelated disorder peak widths are independent of angle (Stroud & Millane, 1996). X-ray diffraction experiments have shown that correlated disorder is present in a variety of disordered crystalline materials (Alexander, 1969; Hosemann & Hindeleh, 1995; Welberry & Butler, 1995).

Two principal models have been used to describe disordered crystalline materials, the paracrystal and the perturbed lattice, both of which incorporate correlated disorder. The paracrystal model was developed by Hosemann and co-workers (Hosemann & Bagchi, 1962) and has been widely used to analyze diffraction from disordered materials such as polymers, glasses and alloys (Hosemann & Hindeleh, 1995), and is based on a statistical description in terms of the lengths and directions of the nearest-neighbor inter-site vectors in a distorted lattice. The perturbed lattice, on the other hand, describes a distorted lattice in terms of the displacements of its sites away from those of a periodic reference lattice (Welberry *et al.*, 1980; Welberry, 1985; Stroud & Millane, 1996). Both the paracrystal and the perturbed lattice models are well defined in one dimension but are well defined only under restricted conditions in more than one dimension (Welberry, 1985). In particular, in a two- or three-dimensional lattice there are many more cell edges (with which the random variables of the paracrystal are associated) than lattice points, implying that conditional dependencies must be imposed on the distributions (Hammersley, 1967). The perturbed lattice model circumvents this difficulty by working with the lattice points rather than the vectors between them, although there are still difficulties with devising general two- or three-dimensional perturbed lattices (Welberry & Carroll, 1982). Our focus here is on the paracrystal model.

A number of paracrystal models have been described in two dimensions. The simplest and most widely used is the *ideal paracrystal* (Hosemann & Bagchi, 1962). The two-dimensional ideal paracrystal has well defined statistics and can be constructed using two one-dimensional paracrystals (in the plane), each oriented along the primary axes of an underlying regular two-dimensional lattice. The ideal paracrystal is then formed by convolving these two one-dimensional paracrystals with each other. The resulting distorted two-dimensional lattice is made up of cells that are parallelograms and therefore represents a rather restricted, and unrealistic, form of disorder. A more general and potentially more realistic model is the *spiral paracrystal* (Janke & Hosemann, 1978; Hosemann *et al.*, 1981). The cell shape of the spiral paracrystal is not restricted to a parallelogram; however, a disadvantage is that the statistics of the distortions are not well defined, and an analytic expression cannot be obtained for its diffraction. The spiral paracrystal is an interesting and potentially useful model however.

A characteristic of paracrystal models is that the variance of the distance from the origin to a lattice point increases without bound as the distance from the origin increases. This is of no particular concern for the one-dimensional paracrystal; however, for two- or three-dimensional paracrystals, it is problematic because it can lead to large fluctuations in the lengths of the edges of a single cell, and thence to a very distorted cell, as the distance from the origin increases. This problem has been circumvented by proposing that a paracrystalline domain grows only until the fluctuations of the cell edges reach a certain value (Hosemann, 1975; Baltá-Calleja & Hosemann, 1980) and no further growth occurs. Since the variance of the fluctuations depends on the degree of disorder between adjacent sites and the size of the domain, this requirement gives an implicit relationship between the size of a paracrystalline domain (crystallite size) and the degree of disorder within the lattice. Such a relationship has been observed experimentally from analysis of X-ray diffraction peak breadths, from which one can estimate average crystallite size and paracrystalline disorder (Hosemann *et al.*, 1981), and has been called the '$\alpha^*$ rule' (Baltá-Calleja & Hosemann, 1980). Current explanations of the $\alpha^*$ rule are based on the one-dimensional paracrystal and are not particularly convincing (Hosemann, 1975; Baltá-Calleja & Hosemann, 1980; Hosemann & Hindeleh, 1995). We examine here a more detailed model of the relationship between crystallite size and paracrystalline disorder that is based on the spiral paracrystal.

## 2. The paracrystal and the $\alpha^*$ rule

The one-dimensional paracrystal is a sequence of points distributed along a line that represents a distorted one-dimensional lattice. The distorted lattice is defined only by specification of the probability density function (usually taken to be normal) of the distances $d_j = x_{j+1} - x_j$ between nearest-neighbor lattice points, where $j$ indexes the lattice points and $x_j$ is the coordinate of the $j$th point. The $d_j$ are taken to be independent. Properties of the one-dimensional paracrystal are described elsewhere (Hosemann & Bagchi, 1962; Mu, 1998; Millane & Eads, 2000). For our purposes, an important result is that the variance of the distance $x_{j+k} - x_j$ between $k$th nearest neighbors is equal to $k\sigma^2$, where $\sigma^2$ is the variance of the distance between first nearest neighbors (Millane & Eads, 2000).

A simple, but not particularly realistic, model of a two-dimensional paracrystal is a set of parallel one-dimensional paracrystals. If these one-dimensional paracrystals are in register at say $j = 0$, then the variance of the $x$ component of the distance between the $j$th lattice points in two adjacent one-dimensional paracrystals is $2j\sigma^2$. Since these two points belong to the same cell in the two-dimensional paracrystal, $2j\sigma^2$ represents the average degree of distortion of the cell. If we accept that there is an upper limit to how much a cell can be distorted, then there is a limit on $2j\sigma^2$, or on $j$, *i.e.* there is an upper bound on the number of lattice points in the one-dimensional paracrystals. We denote this upper bound by $N$, which represents the average lateral dimensions of a paracrystalline domain, and we refer to it as the crystallite size. The above argument implies that $N$ is proportional to $1/\sigma^2$, and this is often written as

$$N = \alpha^{*2}\sigma^{-2}, \tag{1}$$

where $\alpha^*$ is a constant, and (1) is called the $\alpha^*$ rule (Baltá-Calleja & Hosemann, 1980). The above argument is the current explanation of the $\alpha^*$ rule (Hosemann, 1975; Baltá-Calleja & Hosemann, 1980; Hosemann & Hindeleh, 1995), but it is based on a quite unrealistic model of a two-dimensional paracrystal. Experimental measurements of X-ray diffraction peak widths allow $N$ and $\sigma$ to be estimated, and results show that (1) is satisfied reasonably well for a variety of materials with $\alpha^* \approx 0.15$ (Baltá-Calleja & Hosemann, 1980). It is therefore of interest to see if (1) can be explained on the basis of a more realistic model of a two-dimensional paracrystal. The ideal paracrystal is not particularly realistic, however, as described above, and, since it is constructed from two one-dimensional paracrystals, fluctuations in the shapes of the cells do not increase as much as they would in a more realistic paracrystal. We have therefore chosen the spiral paracrystal to investigate the $\alpha^*$ rule.

## 3. The spiral paracrystal

### 3.1. Construction

The spiral paracrystal is constructed as follows (Janke & Hosemann, 1978; Hosemann *et al.*, 1981). We consider a square (undistorted) lattice and normalize the lattice spacing to unity. The spiral paracrystal is constructed following a spiral path, beginning at the origin, as shown in Fig. 1. The lattice points are divided into two kinds; edge points (open circles in Fig. 1) and corner points (filled circles in Fig. 1) on the spiral. The positions of these two kinds of points are determined slightly differently. The position of an edge point is determined relative to its two nearest neighbors in the existing lattice. Two preliminary points (⊗ in Fig. 1) for a new edge

point are generated based on each of the two nearest neighbors. The $x$ and $y$ components of the vector from a neighbor to the corresponding preliminary point are chosen randomly from two normal distributions of variance $\sigma^2$ (which defines the degree of distortion of the lattice). The mean of one of these distributions is $\pm 1$ and the mean of the other is zero, the actual values used being those that put the preliminary points in the appropriate positions. Since the two preliminary points will not in general coincide (Fig. 1), the position of the new point is chosen such that its distance to each neighbor is equal to the distance from that neighbor to its preliminary point. This construction is illustrated in Fig. 1 and can be described by drawing two circles with centers at each neighbor and with radii ($l_1$ and $l_2$ in Fig. 1) equal to the distance to the corresponding preliminary point. The new point is then located at the intersection of the two circles (choosing the appropriate one of the two intersections). Note that the only purpose of the preliminary points is to determine the distances $l_1$ and $l_2$. The corner points have only one nearest neighbor (Fig. 1) and the single preliminary point, generated as described above, is used as the new point. The spiral paracrystal is constructed by sequentially adding edge and corner points, following the spiral path as shown in Fig. 1.

### 3.2. Growth termination conditions

Distortions in the spiral paracrystal are cumulative since each lattice point is added relative to the positions of previous points. The average distortion of the cells therefore tends to increase with increasing distance from the origin of the lattice, and the model can be used to investigate the relationship between crystallite size and degree of distortion in a more realistic way than for the one-dimensional paracrystal. We assume that growth of the spiral paracrystal stops when a new point to be added leads to a new cell that is too distorted. We refer to conditions under which growth stops as *termination conditions*. Termination of growth defines the size of the paracrystalline domain (crystallite). The average crystallite size can be calculated by averaging over many realizations of such lattices.

Janke & Hosemann (1978) and Hosemann *et al.* (1981) described a termination condition as follows. With reference to Fig. 1, the position of a new edge point is not defined if the two circles centered on the two nearest neighbors do not intersect. They define growth as stopping the first time that this occurs. Inspection of the figure shows that this termination condition is

$$l_1 + l_2 < d \quad \text{or} \quad |l_1 - l_2| > d, \tag{2}$$

where $d$ is the distance between the two nearest neighbors, and growth of a lattice terminates the first time that (2) is satisfied. Note that $d$ is the length of the diagonal of the cell that is to be added to the lattice. Equation (2) will tend to be satisfied when $d$ takes on extreme (large or small) values.

We also consider here a simpler termination condition related to the deviation of the length of the diagonal of a new cell from the nominal value for an undistorted cell ($2^{1/2}$ in our case). The second termination condition is then defined by

$$|d - 2^{1/2}| > 2^{1/2}\beta, \tag{3}$$

*i.e.* growth stops when the length of the diagonal of a cell deviates from its nominal value by a fraction $\beta$, which can be treated as a parameter. In this case, condition (2) is ignored when building the lattice by repeatedly generating preliminary points if necessary until a valid new point is obtained.

## 4. Simulations

Janke & Hosemann (1978) and Hosemann *et al.* (1981) generated a spiral paracrystal using the termination condition (2) described above and noted that its size satisfied the $\alpha^*$ rule. However, this was a single simulation for a single value of $\sigma$ and so does not provide a definitive result. Our objective here

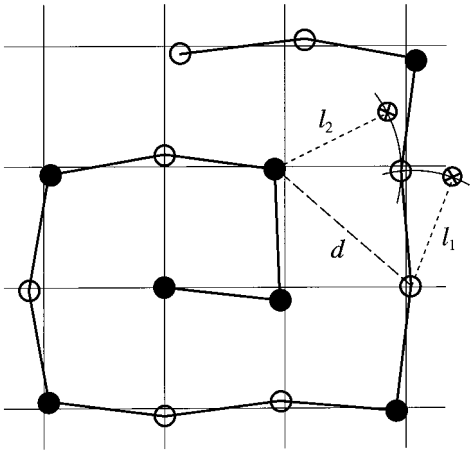


**Figure 1**
Construction of the spiral paracrystal (see text). Edge points (open circles), corner points (filled circles) and preliminary edge points (⊗).

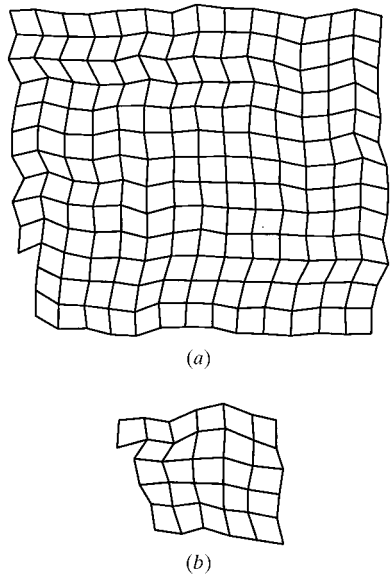


**Figure 2**
Examples of simulated spiral paracrystals for (*a*) $\sigma = 0.05$ and (*b*) $\sigma = 0.10$.

is to examine the crystallite size–disorder relationship for a range of values of $\sigma$ and with appropriate averaging over an ensemble of spiral paracrystals.

Spiral paracrystals were generated as described above for values of $\sigma$ between 0.01 and 0.2. Examples of two such lattices are shown in Fig. 2. Both (2) and (3) were used as termination conditions. For each value of $\sigma$, 5000 lattices were generated and the crystallite sizes, denoted by $N$ and defined as the square root of the number of points in the lattice, were averaged over all the lattices. The average size so obtained is denoted by $\bar{N}$. The 5000 lattices were also divided into 10 groups of 500, $\bar{N}$ calculated for each group, and the standard deviation of $\bar{N}$ calculated. The standard deviation of $\bar{N}$ was less than 2% in all cases. Plots of $\bar{N}$ *versus* $\sigma$ for the two termination conditions are shown in Fig. 3. The $\alpha^*$ rule for $\alpha^* = 0.15$, and the data in Fig. 4 of Hosemann *et al.* (1981) are also shown in the figure. The value $\beta = 0.40$ in (3) was chosen to minimize the r.m.s. difference between $\bar{N}$ and the data in Fig. 3.

Inspection of Fig. 3 shows that the spiral paracrystal models with both termination conditions provide reasonable fits to the data and are similar to the $\alpha^*$ rule. The termination condition (2) appears to provide an upper bound to $\bar{N}$, rather than average values over the data, however. Termination condition (3) provides a good overall fit to the data. Fitting power-law relationships between $\bar{N}$ and $\sigma$ to the curves in Fig. 3 based on the spiral paracrystal gives

$$\bar{N} = 1.0 + 0.11\sigma^{-1.8} \qquad (4)$$

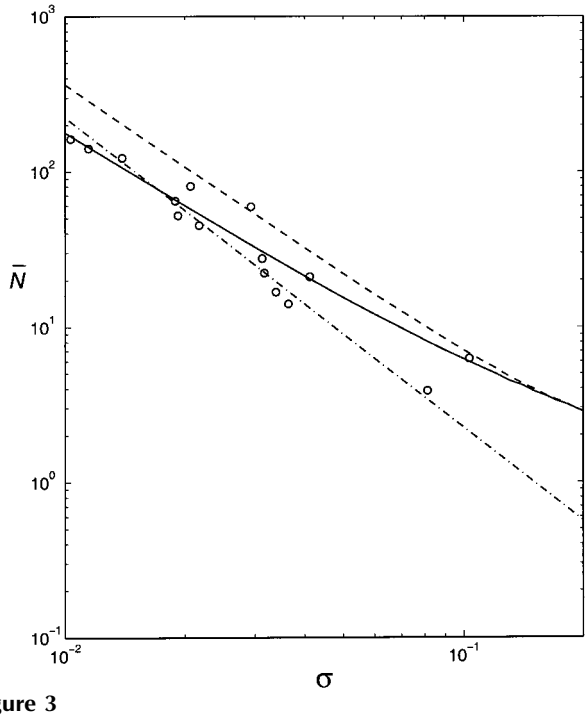


**Figure 3**
Average crystallite size, $\bar{N}$, *versus* $\sigma$ for the spiral paracrystal with termination condition (2) (dashed line), termination condition (3) with $\beta = 0.40$ (solid line), and the $\alpha^*$ rule with $\alpha^* = 0.15$ (dot-dashed line). Experimental data from Fig. 4 of Hosemann *et al.* (1981) are shown by the circles.

for termination condition (2),

$$\bar{N} = 1.4 + 0.12\sigma^{-1.6} \qquad (5)$$

for termination condition (3) with $\beta = 0.40$. The fits of (4) and (5) to the simulations are essentially perfect. Note the similarity of (4) and (5). These relationships are similar to the $\alpha^*$ rule (1). However, a disadvantage of the $\alpha^*$ rule is that it predicts non-physical values $\bar{N} < 1$ for large values of $\sigma$. Relationships (4) and (5) satisfy $N > 1$ however.

The simulations described above can be used to calculate the distribution of crystallite sizes as a function of $\sigma$. The distributions were calculated [based on (3) with $\beta = 0.40$] and are shown, normalized by $\bar{N}$, in Fig. 4(*a*) for four values of $\sigma$. Inspection of the figure shows that the distributions of crystallite sizes are approximately normal, except for large $\sigma$ and broaden (when normalized to $\bar{N}$) with increasing $\sigma$. The standard deviations of the distributions, denoted by $\Sigma$, were also calculated and are shown in Fig. 4(*b*) (also normalized by $\bar{N}$). The standard deviation of $N/\bar{N}$ increases with $\sigma$, *i.e.* there is a wider variety of relative crystallite sizes (larger $\Sigma/\bar{N}$) for larger disorder, as might be expected.

## 5. Conclusions

Previous theoretical explanations of the experimentally observed inverse relationship between crystallite size and degree of disorder in paracrystalline materials have been either unsatisfactory or incomplete. A more complete quantitative explanation based on the two-dimensional spiral paracrystal has been described and provides a more satisfac-

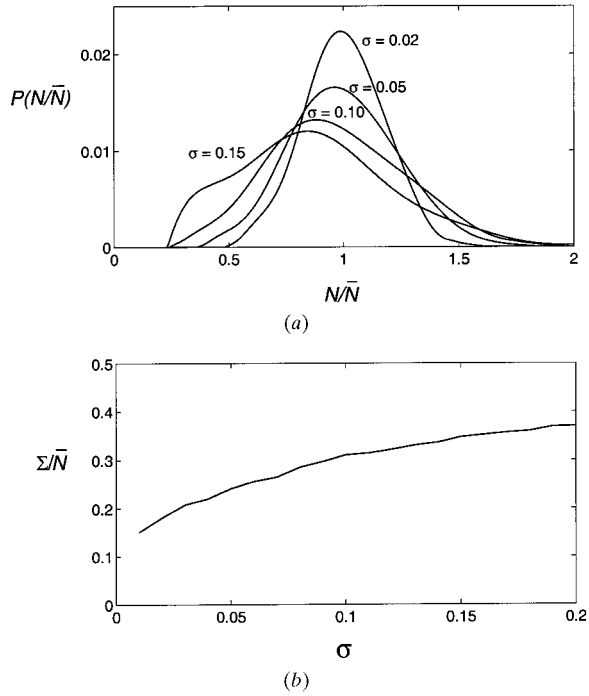


**Figure 4**
(*a*) Crystallite-size distributions (normalized to $\bar{N}$) and (*b*) their standard deviations as a function of $\sigma$.

tory explanation of this relationship. The model leads to relationships between mean crystallite size and disorder that are similar to the $\alpha^*$ rule and provide a reasonably good fit to observed data. The model also allows one to propose crystallite-size distributions as a function of disorder.

We are grateful to the US National Science Foundation for support (DBI-9722862).

## References

Alexander, L. E. (1969). *X-ray Diffraction Methods in Polymer Science*, ch. 7. New York: Robert E. Krieger.
Baltá-Calleja, F. J. & Hosemann, R. (1980). *J. Appl. Cryst.* **13**, 521–523.
Hammersley, J. M. (1967). *Proc. 5th Berkeley Symp. on Mathematical Statistics and Probability*, Vol. 3, pp. 89–118. Berkeley: University of California Press.
Hosemann, R. (1975). *J. Polym. Sci.* **50**, 265–281.
Hosemann, R. & Bagchi, S. (1962). *Direct Analysis of Diffraction by Matter.* Amsterdam: North-Holland.
Hosemann, R. & Hindeleh, A. (1995). *J. Macromol. Sci. Phys.* B**34**, 327–356.
Hosemann, R., Vogel, W., Weick, D. & Baltá-Calleja, F. J. (1981). *Acta Cryst.* A**37**, 85–91.
Janke, M. & Hosemann, R. (1978). *Prog. Colloid Polym. Sci.* **64**, 226–231.
Millane, R. P. & Eads, J. L. (2000). *Acta Cryst.* A**56**, 497–506.
Millane, R. P. & Stroud, W. J. (1991). *Int. J. Biol. Macromol.* **13**, 202–208.
Mu, X. Q. (1998). *Acta Cryst.* A**54**, 606–616.
Stroud, W. J. & Millane, R. P. (1995). *Acta Cryst.* A**51**, 790–800.
Stroud, W. J. & Millane, R. P. (1996). *Proc. R. Soc. London Ser. A*, **452**, 151–173.
Welberry, T. R. (1985). *Rep. Prog. Phys.* **48**, 1543–1593.
Welberry, T. R. & Butler, B. D. (1995). *Chem. Rev.* **95**, 2369–2403.
Welberry, T. R. & Carroll, C. E. (1982). *Acta Cryst.* A**38**, 761–772.
Welberry, T. R., Miller, G. H. & Carroll, C. E. (1980). *Acta Cryst.* A**36**, 921–929.